

Hyperglycaemia and aberrated insulin signalling stimulate tumour progression via induction of the extracellular matrix component hyaluronan

Sören Twarock , Christina Reichert, Ulrike Peters, Daniel J. Gorski, Katharina Röck and Jens W. Fischer

Institut für Pharmakologie und Klinische Pharmakologie, Universitätsklinikum der Heinrich-Heine-Universität, Düsseldorf, Germany

Epidemiological studies have detected a higher incidence of various tumour entities in diabetic patients. However, the underlying mechanisms remain insufficiently understood. Glucose-derived pericellular and extracellular hyaluronan (HA) promotes tumour progression and development. In our study, we tested the hypothesis that a diabetic metabolic state, characterised by hyperglycaemia and concomitant aberrant insulin signalling, stimulates tumour progression via the induction of HA synthesis. In a streptozotocin-induced diabetic nude mouse tumour xenograft model, hyperglycaemia and lack of insulin caused an increased formation of tumour-associated HA-matrix, which in turn accelerated tumour progression and neoangiogenesis. This process was effectively attenuated by treatment with 4-methylumbelliferone, a pharmacological inhibitor of HA-synthesis. To define the mechanisms behind these *in vivo* observations, we investigated the impact of hyperglycaemia and insulin on the glucose metabolism in oesophageal squamous cell cancer cells (ESCC). Hyperglycaemia induced HA synthesis while insulin diminished HA production by directing glucose metabolites to glycolysis. *Vice versa*, inhibition of glycolysis, either by knock-down of the glycolytic key enzyme phosphofructokinase or by an experimental abrogation of insulin signalling (knockdown of the insulin receptor and long-term treatment with insulin) augmented HA synthesis. Consequently, these processes induced invasion, anchorage-independent growth and adhesion of ESCC to endothelial cells *in vitro*. Thus, the cellular shift in glucose usage from catabolism of glucose to anabolism of HA driven by hyperglycaemia and insulin resistance may represent an important link between diabetes and cancer progression. Hence, therapeutical inhibition of HA synthesis may represent a promising approach for tumour treatment in diabetic patients.

Introduction

Diabetes is a widespread disease and is accountable for a plethora of sequelae and pathologies. In recent epidemiological studies, both Type 1 and Type 2 diabetes have been linked to an

Key words: diabetes, oesophageal cancer, extracellular matrix, hyaluronan, 4-methylumbelliferone, pharmacological therapy

Abbreviations: ESCC: oesophageal squamous cell cancer cells; FACE: fluorophore-assisted carbohydrate electrophoresis; G6P: glucose-6-phosphate; HA: hyaluronan; HCAECs: human coronary artery endothelial cells; HAS: HA synthase; IGF: insulin-like growth factor; INSR: insulin receptor; INSR- β : insulin receptor subunit beta; IRS-1: insulin receptor substrate 1; MAPK: mitogen-activated protein kinase; 4-MU: 4-methylumbelliferone; PFKM: phosphofructokinase M.; UDP: uridine diphosphate; TUNEL: TdT-mediated dUTP-biotin nick end labeling

Additional Supporting Information may be found in the online version of this article.

DOI: 10.1002/ijc.30776

History: Received 6 Oct 2016; Accepted 26 Apr 2017; Online 10 May 2017

Correspondence to: Sören Twarock, Institut für Pharmakologie und Klinische Pharmakologie, Universitätsklinikum der Heinrich-Heine-Universität, Düsseldorf, Germany, E-mail: soeren.twarock@uni-duesseldorf.de; Tel. +49-211-81-12500, Fax +49-211-81-14781

increased prevalence of several types of tumour entities¹ including oesophageal cancer.² Furthermore, some malignancies, such as hepatocellular carcinoma, respond poorly to chemotherapeutic intervention in diabetic patients.³ The mechanisms underlying these findings are insufficiently understood but presumably involve high glucose uptake by tumour cells, anabolic actions of insulin and the production of inflammatory cytokines by adipose tissue.⁴ Increased uptake and metabolism of glucose, termed the Warburg effect, is regarded as an import hallmark of cancer cells.^{5,6} These processes provide an increase in energy substrates and further fuel biomass synthesis.⁷ Besides an indirect increase in insulin and insulin-like growth factor (IGF), hyperglycaemia can directly induce pathways that promote proliferation, antiapoptosis and invasion.⁸ Furthermore, hyperglycemia causes epigenetic changes, which result in a prolonged activation of tumour cell proliferation.⁹ However, many aspects of the direct effects of hyperglycemia on cancer cell progression need further investigation.¹⁰

Oesophageal cancer occurs with approximately equal probability as either adenocarcinoma or squamous cell carcinoma (ESCC). It is the sixth leading cause of cancer-related deaths worldwide, with a rapid increase in the last decades. Despite technical advances in surgery, intensified use of neo-adjuvant chemoradiotherapy, and the introduction of new cytotoxic drugs, the mortality rate associated with

What's new?

The mechanisms by which hyperglycemia and other diabetes-related factors promote tumourigenesis are not fully understood, and while glucose metabolites and glycolytic precursors are implicated, their involvement remains largely undefined. In this investigation of hyperglycemia and glucose metabolism in esophageal squamous cell cancer cells, abrogated insulin signalling was found to work in combination with hyperglycemia to redirect glucose usage from glycolytic catabolism to anabolism of HA, an extracellular matrix polysaccharide synthesized from precursors in the first stages of glycolysis. Augmented HA facilitated the development of a malignant phenotype and tumour progression. Its synthesis was blocked by the inhibitor 4-methylumbelliferone.

oesophageal cancer is similar to its incidence rate. The 5-year survival rate ranges from 15 to 25%.¹¹

HA has been identified as a determinant of cancer progression, neoangiogenesis, metastasis and resistance to chemotherapy.^{12,13} Of note, HA is an important protumourigenic component of the microenvironment of oesophageal cancer.¹⁴ HA is an unbranched high-molecular-weight polysaccharide, composed of D-glucuronic acid and D-N-acetylglucosamine disaccharide units, and is exclusively synthesised from precursors that are generated during the first steps of glycolysis. The production of HA is facilitated by three isoforms of the HA synthase family (HAS1–3), which are located at the plasma membrane and extrude HA into the extracellular space.¹⁵ HA synthesis can be blocked by the HAS inhibitor 4-methylumbelliferone (4-MU).¹⁶

Both hyperglycaemia and elevated HA synthesis have been shown to enhance tumour progression, metastasis and chemotherapy resistance.^{10,12,13} Insulin plays a major role in diabetes as well as the cell's glucose metabolism, especially by governing glucose metabolites to distinct downstream pathways.¹⁷ Hence, in the study reported here we addressed the question of whether diabetes-associated hyperglycaemia and aberrant insulin signalling may account for the overproduction of tumour-promoting HA in ESCC cells and whether this process is mediated by a crosstalk between glycolysis and HA synthesis. *In vivo*, in a diabetic nude mouse tumour xenograft model, we investigated the influence of this process on tumour progression and tested systemic HA synthesis inhibition as a potential treatment option. Thus, we evaluated the efficacy of 4-MU, an orally available HAS inhibitor with documented safety in humans, for the treatment of diabetes-induced cancer growth.

Material and Methods**Reagents and substances**

Unless denoted otherwise, all reagents were obtained from Sigma–Aldrich (St. Louis, MO).

Cell culture

The primary ESCC lines OSC1 and OSC2 were isolated and kindly provided by M. Sarbia.¹⁸ KYSE-30, KYSE-270, KYSE-410 and KYSE-520 cells were obtained from DSMZ (Braunschweig, Germany). The identity of the four KYSE cell lines was validated by short tandem repeat (STR) analysis. Briefly, multiplex PCR reactions were performed by amplifying

genomic DNA using Identifier-1 Kit (ABI, Waltham, MA) and ESI17 Kit (Promega, Fitchburg, WI). Analyses were performed in the Institut of Forensic Medicine, University Hospital Duesseldorf. The identity of OSC1 and OSC2 was validated by karyotype analysis in the Institute of Human Genetics, University Hospital Duesseldorf. The cells were maintained as previously described.¹⁹ Insulin resistance was induced *in vitro* by incubation with 100 nM insulin and high-glucose media for 3 days, as previously described.²⁰ HAS activity was inhibited by treatment with 4-MU, sodium salt (0.3 mM, 24 hr).

Quantitative real-time reverse-transcriptase polymerase chain reaction

Total RNA from cultured cells was isolated, reverse transcribed and analysed by qRT-PCR as described previously.¹⁹ The following primers were used (gene of interest, sense and antisense sequences): INSR, 5'-GCTGCCACCAGTACGTCATT-3' (sense), 5'-GTCGATGGTCTTCTCGCCTT-3' (antisense); PFKM, 5'-TCATGACCCATGAAGAGCAC-3' (sense), 5'-GCACCGGTGAAGATACCAAC-3' (antisense); HAS1, 5'-TTCTTCAGTCTGGACATATTTGGGA-3' (sense), 5'-CCTGATCACACAGTAGAAATGG-3' (antisense); HAS2, 5'-GTGGGGAAGAATCAAACATTTAAGA-3' (sense), 5'-AATGCATCTTGTTCAGCTCTTG-3' (antisense); HAS3, 5'-GGAGGAGGATCCCCAAGTAG-3' (sense), 5'-CTGCTCAGGAAGGAAATCCA-3' (antisense); GLUT1, 5'-CTGAAGTCGCACAGTGAATA-3' (sense), 5'-TGGGTGGAGTTAATGGAGTA-3' (antisense); GLUT4, 5'-CCTGGTCCTTGCTGTGTTCT-3' (sense), 5'-CCAGCCACGTCTCATTGTAG-3' (antisense).

Immunoblot analysis

Immunoblots were performed as previously described.¹⁹ Primary antibodies against the following target proteins were used: IRS-1 (D23G12), p-IRS1 (Ser307) from Cell Signaling Technology (Danvers, MA); p-Tyr (PY99, Santa Cruz, Dallas, TX); insulin receptor beta (ab69508; Abcam, Cambridge, UK) and beta tubulin I (T7816; Sigma–Aldrich). Detection was performed with IR fluorescent secondary antibodies (IrDye; LI-COR, Lincoln, NE) using an Odyssey Infrared Imaging System (LI-COR).

Transfection and gene silencing

Knockdown of the genes of interest was achieved by lipotransfection of siRNAs or scrambled control siRNA (Qiagen, Hilden,

Germany) with Lipofectamine RNAiMaxx (Thermo Fisher, Waltham, MA) according to the manufacturer's instructions. The following siRNAs were used (gene of interest, Qiagen order numbers): INSR SI00004508, SI00004515, PFKM SI00604835, SI00604828, HAS3 SI04201246, SI00433895, AllStars Negative Control siRNA SI03650318.

HA measurement

HA in supernatants was measured by a commercially available HABP immunoaffinity assay (Corgenix, Broomfield, CO). For detection of HA newly synthesised from glucose, a radioactive HA assay was used. This assay was performed analogously to HA purification as described in literature.²¹

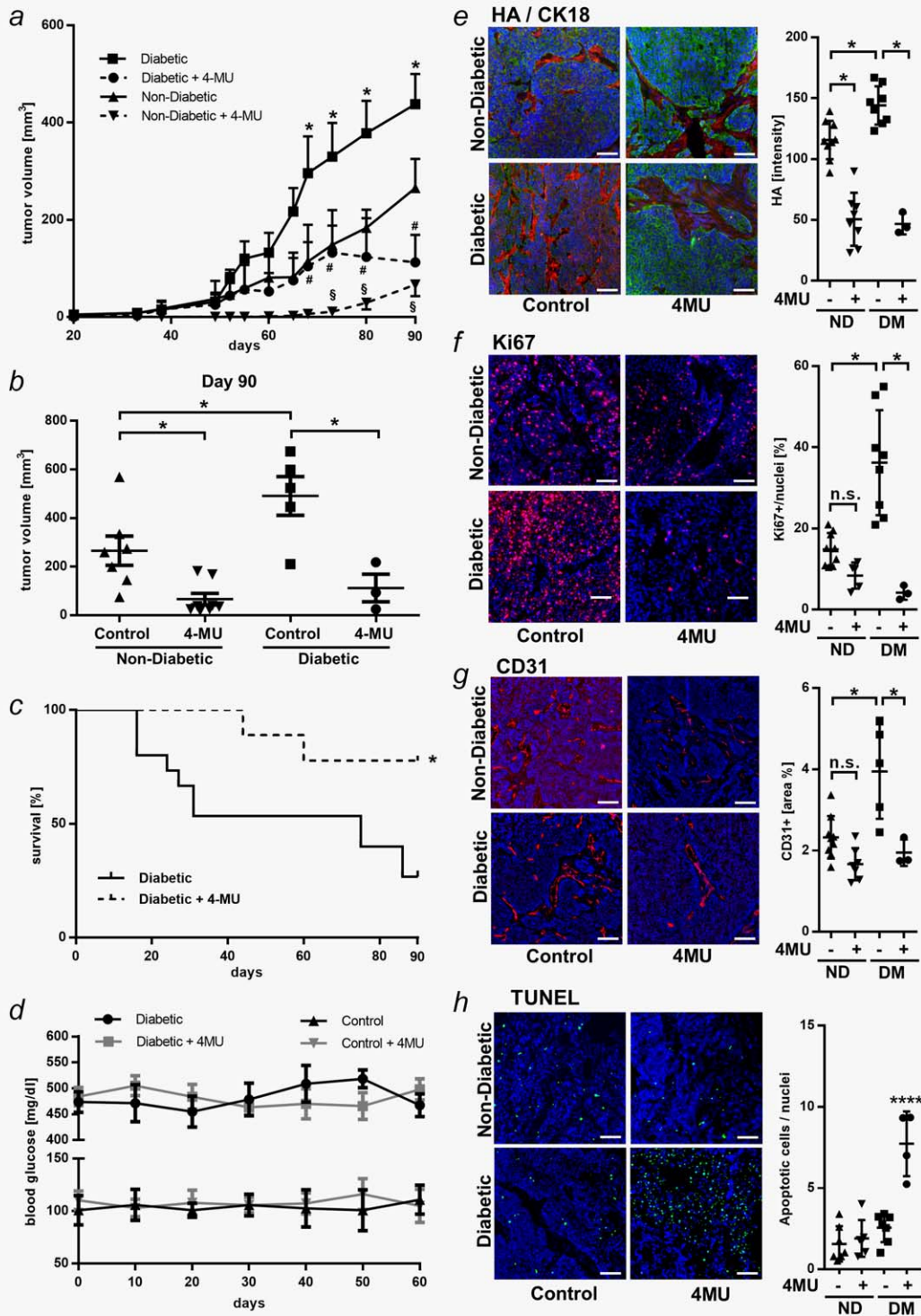


Figure 1.

Briefly, cells were incubated with [14C]-labelled glucose (20 μ Ci/ml; Hartmann Analytic, Braunschweig, Germany). Next, pronase (200 μ m/ml) was used to break up HA protein complexes, and half of the extract was digested with bovine hyaluronidase (10 U/ml, H3506, Sigma–Aldrich). To remove any unincorporated radiolabels, low-molecular-weight sugars and peptides, both samples were separately applied to a DEAE-Sephacel column (GE Healthcare, Little Chalfont, UK). Eluted HA was mixed with scintillation fluid (Rotiszint; Roth, Karlsruhe, Germany) and counted in a scintillation counter. The amount of HA was defined as the number of hyaluronidase-susceptible counts per minute (cpm) normalised to the protein content of the cell layer, as determined by Bradford assay.

Quantification of glucose metabolites

Intracellular glucose-6-phosphate and pyruvate as well as extracellular lactate concentrations were quantified with commercially available colorimetric assays (Lactate Assay Kit II, Glucose-6-Phosphate Assay Kit; Sigma–Aldrich and Pyruvate Assay Kit; abcam) according to manufacturer's instructions. Intracellular uridine diphosphate (UDP)-glucose/galactose, UDP-glucuronic acid and UDP-N-acetylglucosamine were quantified by fluorophore-assisted carbohydrate electrophoresis (FACE) as previously described.²² Briefly, cultures were given low or high glucose containing media for 24 hr. Cell layers were collected on ice and sonicated, nucleotide sugars were then purified using solid phase extraction with ENVI-Carb SPE columns (Sigma–Aldrich). Monosaccharides were released from nucleotide residues by mild acid hydrolysis and conjugated to 2-aminoacridone (Invitrogen) before separation by gel electrophoresis. Samples were run alongside a control ladder of glucose, N-acetylglucosamine and glucuronic acid (Sigma–Aldrich). Band intensities were then integrated using image J and normalized to DNA content determined by a Quant-iT PicoGreen dsDNA Assay Kit (Invitrogen).

Proliferation assay

Proliferation was measured by a ³[H]-thymidine assay as previously described.¹⁹

Adhesion assay

The impact of HA on the adhesion of cancer cells to endothelial cells by was assessed as previously described²³ but with microscopic analysis instead of a radioactive assay. In detail, human coronary artery endothelial cells (HCAECs; Promocell, Heidelberg, Germany) were grown to confluence in monolayers in a 12-well plate. OSC1 cells were labelled with calcein (1 μ M) for 20 min and were then seeded at a density of 5×10^4 cells per well on top of the confluent HCAEC monolayers, followed by a 45 min incubation at 4°C with gentle shaking. After washing with PBS, the bound cells were visualised and counted by fluorescence microscopy. To verify HA-dependency of the adhesion, each condition was also treated with hyaluronidase (10 U/ml), and the remaining cells were subtracted.

Matrigel invasion assay

The invasive capability of OSC1 cells over 24 hr was determined with a BD BioCoat Matrigel Invasion Chamber (Cat. 354480; BD Biosciences, Franklin Lakes, NJ) according to the manufacturer's instructions. Cells were counted with a bright-field microscopy after HE staining.

Soft agar assay

The capability for anchorage-independent growth in response to glucose and insulin was assessed as follows: To inhibit adhesion of the cells, the bottom of each well in a 24-well plate was coated with 0.5% Noble agar (BD Difco Agar; BD Biosciences) in RPMI-1640 full medium. OSC1 cells were suspended in a 0.3% agar-RPMI mixture and applied onto the solidified bottom layer. The medium was changed twice weekly, and the assay was analysed after three weeks by

Figure 1. Hyperglycaemia and insulin depletion enhance hyaluronan-dependent tumour progression in a Type 1 diabetes nude mouse xenograft model. (a) Xenograft OSC1 tumour growth over 90 days in diabetic and nondiabetic mice with (dashed lines) or without (solid lines) application of the hyaluronan synthase inhibitor 4-MU. Two-way ANOVA with Tukey's post-test: *, $p < 0.05$ diabetic vs. nondiabetic; #, $p < 0.05$ diabetic vs. diabetic + 4-MU; §, $p < 0.05$ nondiabetic vs. nondiabetic + 4-MU (b) Mean tumour volumes at Day 90. One-way ANOVA with Tukey's post-test of seven nondiabetic, five diabetic, eight nondiabetic + 4-MU and three diabetic + 4-MU tumours. Shown are scatterplots with mean \pm SEM. *, $p < 0.05$ vs. indicated condition. (c) Survival rate of tumour-bearing diabetic nude mice \pm 4-MU within 90 days after xenografting. Fifteen diabetic vs. nine diabetic mice with 4-MU treatment were observed. At the end of the experiment, four diabetic mice and seven 4-MU treated diabetic mice remained alive. Log-rank (Mantel-Cox) test: *, $p < 0.05$. (d) Blood glucose levels. Fifteen nondiabetic (ND), nine diabetic (DM), seven ND + 4-MU and seven DM + 4-MU were observed over 60 days. There was no statistical difference between control and 4-MU treated mice in diabetic and nondiabetic mice, respectively. (e) HA deposition (HABP staining, red) in tumour (cytokeratin 18, CK18, green) and stroma; nuclei (blue, Hoechst). Bar, 100 μ m. Shown are representative images. Quantification of nine nondiabetic (ND), eight diabetic (DM), eight ND + 4-MU and three DM + 4-MU tumours, presented as scatterplot with mean \pm SEM. Statistical significance by one-way ANOVA: *, $p < 0.05$ vs. indicated condition. (f) Proliferation rate in tumour tissue (Ki67 staining, red); nuclei (blue, Hoechst). Bar, 100 μ m. Shown are representative images. Quantification of nine nondiabetic (ND), eight diabetic (DM), five ND + 4-MU and three DM + 4-MU tumours, presented as scatterplot with mean \pm SEM. Statistical significance by one-way ANOVA: *, $p < 0.05$ vs. diabetic condition without 4-MU. (g) Endothelial cell staining (CD31 staining, red) in tumour tissue; nuclei (blue, Hoechst). Bar, 100 μ m. Shown are representative images. Quantification of nine nondiabetic (ND), five diabetic (DM), seven ND + 4-MU and three DM + 4-MU tumours, presented as scatterplot with mean \pm SEM. Statistical significance by one-way ANOVA: *, $p < 0.05$ vs. diabetic condition without 4-MU. (g) Apoptotic cells (TUNEL staining, green); nuclei (blue, Hoechst). Bar, 100 μ m. Shown are representative images. Quantification of seven nondiabetic (ND), six diabetic (DM), seven ND + 4-MU and four DM + 4-MU tumours, presented as scatterplot with mean \pm SEM. Statistical significance by one-way ANOVA: *, $p < 0.05$ vs. all other conditions. [Color figure can be viewed at wileyonlinelibrary.com]

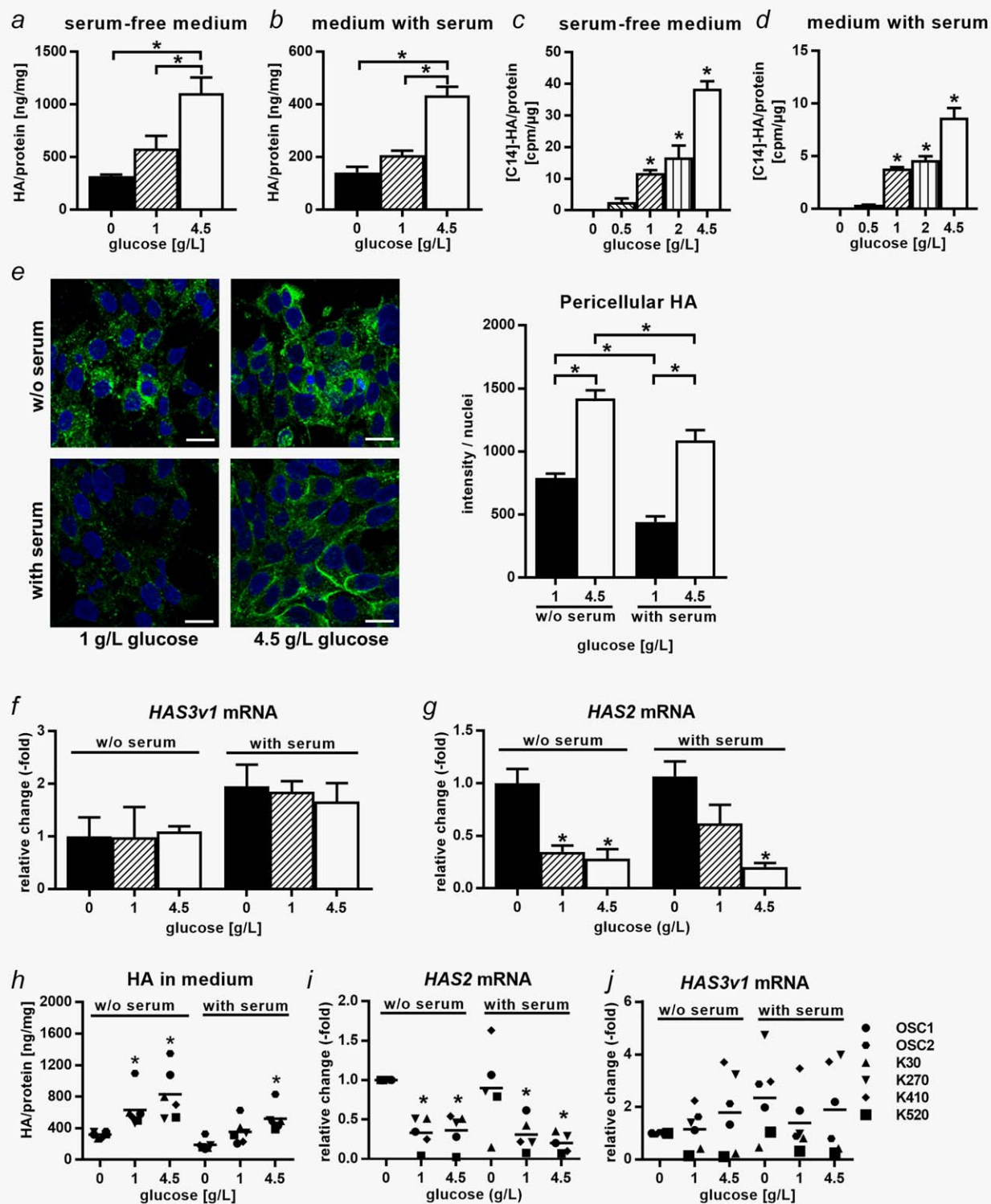


Figure 2. Elevated glucose concentrations facilitate the production of hyaluronan in oesophageal squamous cell carcinoma cell lines. (a, b) Hyaluronan (HA) concentrations in the medium of OSC1 cells normalised to cell layer protein in response to glucose and serum (10% FCS) after 24 hr measured by hyaluronic acid binding protein (HABP) assay. Data are mean \pm SEM from three independent experiments. *, $p < 0.05$ vs. 4.5 g/L glucose. (c, d) [14 C]-glucose integration in HA synthesis normalised to protein of OSC1 cell layer in response to glucose and serum after 24 hr. Data are mean \pm SEM from three independent experiments. *, $p < 0.05$ vs. 0 g/L glucose. (e) Pericellular HA coat of OSC1 cells in response to glucose and serum visualised by HA affinity cytochemistry after 24 hr (HABP, green); nuclei (blue, Hoechst). Scale bar, 10 μ m. Shown are representative results from three independent experiments, mean \pm SEM. *, $p < 0.05$. (f, g) Transcriptional changes in hyaluronan synthase (HAS) 2 and 3v1 mRNA expression in OSC1 cells in response to glucose and serum after 24 hr. HAS1 mRNA was not detectable. Data are mean \pm SEM from three independent experiments. *, $p < 0.05$ vs. 0 g/L glucose. (h, i, j) HA production and HAS mRNA expression in six oesophageal squamous cell carcinoma (ESCC) cell lines: OSC1, OSC2, Kyse 30, Kyse 270, Kyse 410 and Kyse 520 (each cell line represents one n). HAS1 mRNA was not detectable in any cell line. Data are mean \pm SEM from six independent experiments. *, $p < 0.05$, **, $p < 0.01$, ***, $p < 0.001$ vs. 0 g/L glucose. [Color figure can be viewed at wileyonlinelibrary.com]

counting formed colonies larger than 50 μm with a bright-field microscope.

Nude mouse xenograft model and diabetes induction

T cell-immunodeficient male Crl:NU-Foxn1tm mice were obtained from Charles River Laboratories (Wilmington, MA).²⁴ At the age of 6 weeks, a single dose of streptozotocin (240 mg/kg body weight) was injected. When blood sugar levels (tail vein blood glucose test; GlucoSmart, MSP bodmann, Bobingen, Germany) of all mice were verified to be within the target range of 400–600 mg/dl, half of the diabetic and nondiabetic mice was treated with 4-MU (AlfaAesar, ThermoFisher, Waltham, MA), which was pelleted into chocolate flavoured chow at a daily dose of 10 mg/g body weight; the other half of the mice received respective placebo chow. Two days later, 1×10^6 OSC1 cells were injected into both flanks of each mouse. Palpable tumours were detected at approximately Day 20 after xenografting. The mice were observed for a total period of 90 days. The tumour volume was calculated by calliper measurements with the formula $height \times length \times depth \times 0.52$ as described.²⁵ At the end of the observation period, the mice were sacrificed, and tumour xenografts were explanted for histological analysis. The animal experiments were approved by the local animal facility and the corresponding authority (LANUV NRW) and were carried out following the rules and guidelines of the German animal welfare law (Tierschutzgesetz).

Immunostainings

Cryosections (8 μm) were derived from tumour tissue and fixed with formalin. Targets stained comprise HA (HABP; Calbiochem, San Diego, CA), Ki67 (rabbit anti-Ki67; Novus, Littleton), CK18 (guinea pig anti-CK18; Progen, Heidelberg, Germany), CD31 (rat anti-CD31; Abcam) and CD44 (rabbit anti-CD44; Sigma-Aldrich). Apoptotic cells were detected with the Click-it Plus TdT-mediated dUTP-biotin nick end labeling (TUNEL) assay (C10617; Thermo Fisher) according to manufacturer's instructions. Nuclei were counterstained using Hoechst 33342 (Invitrogen, Carlsbad, CA).

Statistical analysis

All datasets were analysed either with ANOVA plus Tukey's or Sidak's *post hoc* test, with Log-rank (Mantel-Cox) test or with Student's *t*-test, as appropriate. All statistical analyses were carried out using GraphPad Prism 6 (Graphpad Software, La Jolla, CA). Data are presented as mean \pm SEM. Statistical significance was set at the level of $p < 0.05$.

Results

Diabetic conditions facilitate HA-mediated tumour progression *in vivo*

To investigate the impact of a diabetic metabolic state on tumour growth and morphology, we developed a Type 1 diabetes nude mouse tumour xenograft model characterised by hyperglycaemia and insulin deprivation: Induction of diabetes

in nude mice by a single injection of streptozotocin yielded blood sugar levels of approximately 400 mg/dl. Starting at around Day 55 after injection of the OSC1 squamous carcinoma tumour cells, the tumour growth curves of nondiabetic and diabetic mice diverged. On Day 90, the tumour volume in diabetic mice was significantly higher than that in nondiabetic mice, which indicates tumour promotion by Type I diabetes conditions. To assess the contribution of HA to this observation and to evaluate pharmacological HA synthesis inhibition as a therapeutic measure, nondiabetic and diabetic mice were fed the HAS inhibitor 4-MU. Of note, 4-MU substantially decreased the rate of tumour growth in diabetic and control mice, however with a more pronounced absolute effect in diabetic mice (Figs. 2a and 2b). Strikingly, 4-MU also increased the mean survival time of the diabetic mice (Fig. 2c). These effects were not accompanied by significant changes in blood glucose concentrations (Fig. 2d). Diabetic conditions resulted in an increase of the total HA deposition in xenograft tumour tissue, which was effectively reduced by treatment with 4-MU (Fig. 2e). Moreover, diabetic conditions strongly increased important histological parameters of tumour progression, i.e., the rate of Ki67-positive proliferating cells (Fig. 2f) and the amount of CD31-positive vessel formation (Fig. 2g). Intriguingly, only under diabetic conditions did 4-MU treatment significantly reduce proliferation (Fig. 2f) and vessel formation (Fig. 2g), and also cause a strong induction of apoptosis (Fig. 2h). The expression of the main HA receptor in ESCC, CD44, was not altered in response to hyperglycemia or 4-MU treatment (supporting information Fig. S1). These results indicate that elevated HA synthesis is of particular importance for tumour growth under diabetic conditions and that 4-MU may be an effective therapeutic drug under these conditions.

Elevated glucose supply augments HA production independently of HAS transcription

In vivo, elevated tumour growth under diabetic conditions was accompanied by increased histological deposition of HA while the inhibition of HA synthesis by 4-MU inhibited tumour growth. To elucidate the mechanism by which diabetic metabolic conditions induce HA synthesis, we performed the following *in vitro* experiments.

As the glycosaminoglycan HA is exclusively synthesised from glucose precursors, we first investigated the influence of glucose supply on HA synthesis. Elevated glucose concentrations caused a dose-dependent increase in HA production by OSC1 cells in medium without (Fig. 3a) and with (Fig. 3b) addition of serum. Strikingly, the presence of serum resulted in lower HA synthesis than did the same glucose concentration in serum-free medium. To verify that the observed increase of HA in the medium was caused by *de novo* synthesis originating from increased glucose uptake, we additionally measured the incorporation of radioactive labelled [14C]-glucose into newly synthesised HA. In agreement with the aforementioned results, radioactive HA also strongly increased with higher glucose

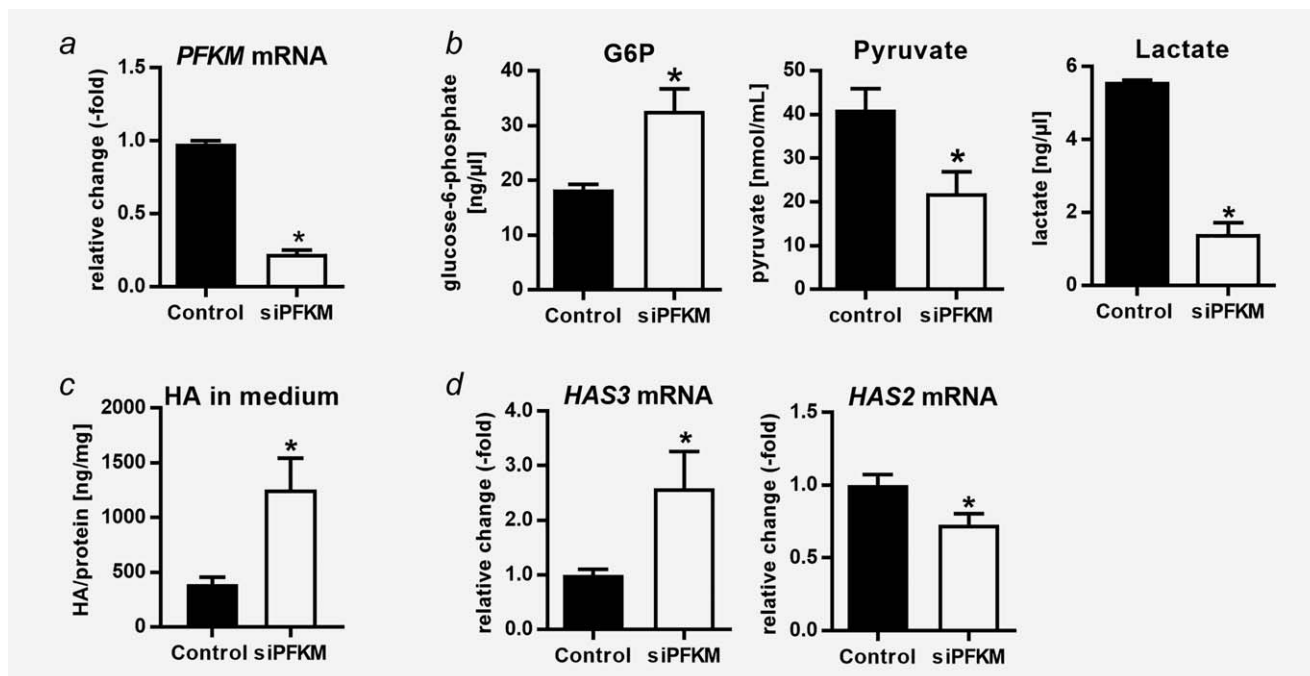


Figure 3. Abrogation of glycolysis directs glucose usage to HA synthesis. (a–d) Changes in the concentration of the glucose metabolites glucose-6-phosphate (G6P, $n = 3$), pyruvate ($n = 6$) and lactate ($n = 3$), in the amount of hyaluronan (HA, $n = 8$) and in the hyaluronan synthase (HAS) mRNA expression (HAS3v1, $n = 8$; HAS2, $n = 6$) in response to abrogation of glycolysis by knockdown of phosphofructokinase M (PFKM) in OSC1 cells with presence of serum after 24 hr ($n = 5$). Data are mean \pm SEM from three to eight independent experiments. *, $p < 0.05$ vs. control.

concentrations in medium without (Fig. 3c) and with (Fig. 3d) serum. Consistently, the pericellular HA coat also increased strongly in response to glucose and also to serum deprivation (Fig. 3e). These results indicate that increased substrate supply is a driving factor for elevated HA synthesis. Interestingly, transcriptional changes in *HAS* genes were not causally involved in this process, since there was no upregulation of *HAS3* (Fig. 3f) and *HAS2* mRNA was even reduced with higher glucose concentrations (Fig. 3g); *HAS1* was not detected. The results observed in OSC1 cells were confirmed in a total of six different ESCC cell lines (OSC1, OSC2, KYSE-30, KYSE-270, KYSE-410 and KYSE-520) (Figs. 3h–3j). To investigate the direct effect of hyperglycemia on HA precursors, sugar nucleotides were quantified by FACE, this showed elevated UDP-glucose/galactose concentrations under stimulation with high glucose media (supporting information Fig. S2a). In this assay, UDP-glucuronic acid (supporting information Fig. S2b) and UDP-N-acetylglucosamine (supporting information Fig. S2c) showed only trends toward increased concentrations, which is likely the result of rapid metabolism by the *HAS* enzymes.

Direct inhibition of glycolysis stimulates hyaluronan synthesis

The observation that HA synthesis is dependent on the availability of glucose precursors raises the question, whether other pathways metabolising these precursors may interfere with HA synthesis. Among these pathways, downstream glycolysis and the pentose phosphate pathway are the most relevant. To

analyse the flux of glucose metabolites, we measured the intracellular concentration of glucose-6-phosphate (G6P), the pivotal upstream metabolite of both HA synthesis and glycolysis, as well as extracellular lactate concentrations as an indicator of glycolytic activity. Silencing of the glycolytic key enzyme phosphofructokinase M (*PFKM*, Fig. 4a) yielded a pronounced disruption of glycolysis, which presented as a strong increase in the intracellular G6P pool and a decrease in pyruvate and lactate concentrations (Fig. 4b). As a result, HA synthesis (Fig. 4c) as well as *HAS3* mRNA were increased while *HAS2* mRNA was reduced (Fig. 4d). The rise in *HAS3* mRNA expression, which was not detected in the experiments involving glucose stimulation (see Figs. 3f and 3j), may be the result of a transcriptional feedback loop between substrate supply to the *HAS* enzymes and *HAS* mRNA expression. Experiments with different *PFKM* knockdown efficiencies show that *HAS3* mRNA expression is positively correlated with *PFKM* knockdown efficiency (supporting information Fig. S3a) while *HAS2* mRNA shows a trend to a negative correlation (supporting information Fig. S3b). Thus, these experiments show a strong cross-talk between those two pathways metabolising glucose, i.e., glycolysis and HA synthesis.

Insulin diminishes HA synthesis by stimulation of glycolysis

The combination of the observations that the presence of serum decreased HA synthesis (see Fig. 3) and that HA synthesis is counteracted by glycolytic activity (see Fig. 4) led us

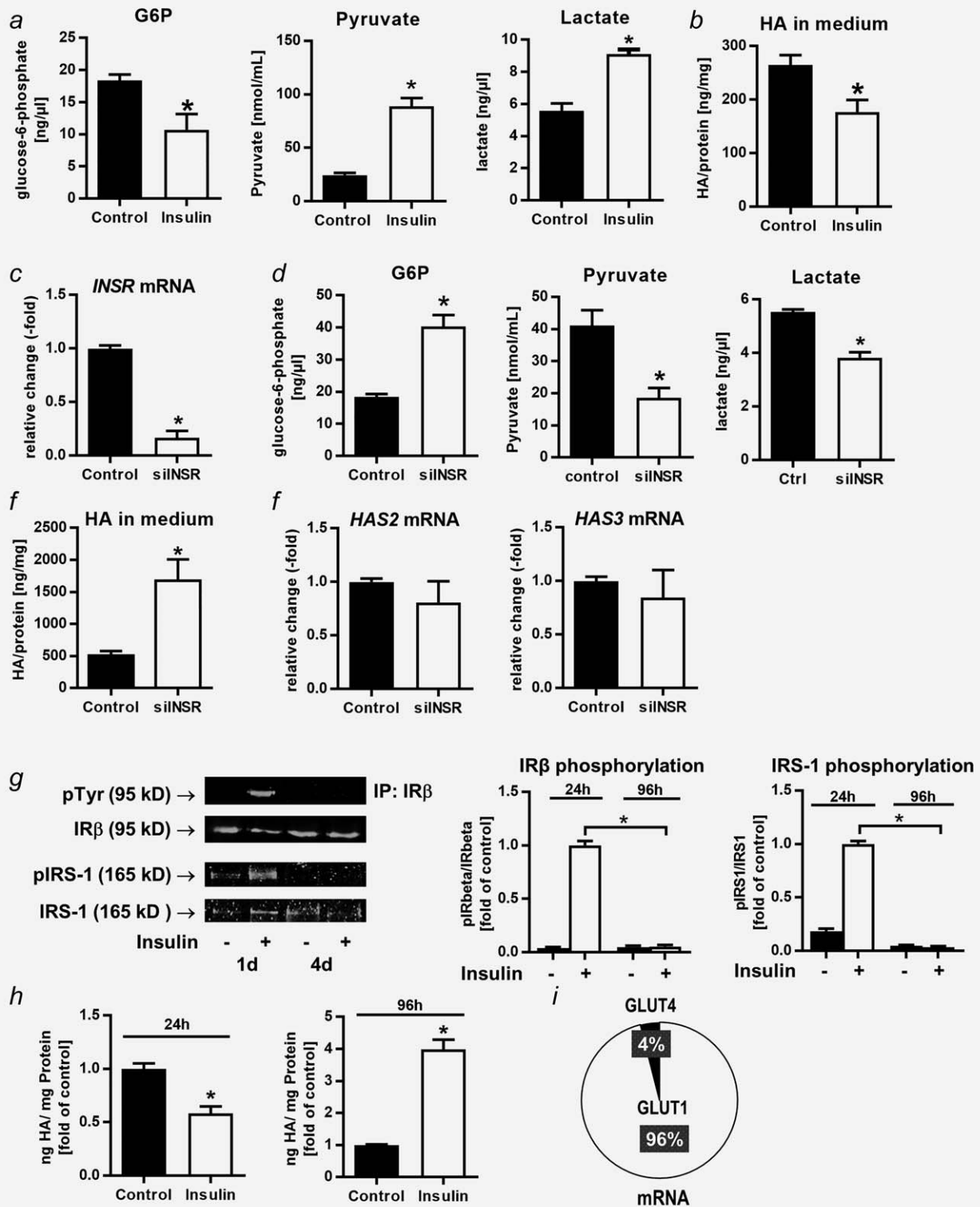


Figure 4. Insulin actions are inversely correlated with hyaluronan synthesis. (a–c) Changes in the concentration of the glucose metabolites glucose-6-phosphate (G6P, $n = 3$), pyruvate ($n = 5$) and lactate ($n = 3$), hyaluronan (HA, $n = 4$) and *HAS* mRNA expression ($n = 3$) in response to stimulation with insulin (50 nM, 24 hr). Data are mean \pm SEM from three to four independent experiments. *, $p < 0.05$ vs. control. (d–i) Effects of insulin receptor (INSR) silencing (INSR mRNA, $n = 4$) on G6P ($n = 3$), pyruvate ($n = 6$) and lactate ($n = 3$) concentrations, hyaluronan synthesis ($n = 4$) and *HAS* mRNA expression ($n = 4$). Data are mean \pm SEM from three to four independent experiments. *, $p < 0.05$ vs. control. (j) Prolonged stimulation with insulin as a model for insulin resistance. Downregulation of insulin receptor activity by long-term (96 hr) insulin stimulation (100 nM), as measured by detection of phosphotyrosine (pTyr)-containing proteins after immunoprecipitation (IP) with anti-insulin receptor subunit beta (IR β) antibody normalised to total IR β protein and detection of phospho-insulin receptor substrate 1 (IRS-1) normalised to total IRS-1. Data are mean \pm SEM from three independent experiments. *, $p < 0.05$ vs. short-term stimulation with insulin. (k) Effects of simulated insulin resistance on HA production. Short-term (24 hr) insulin stimulation vs. long-term (96 hr) insulin resistance. Data are mean \pm SEM from three independent experiments. *, $p < 0.05$ vs. unstimulated control. (l) Expression of glucose transporter 1/4 (GLUT1/4) mRNA in OSC1 cells. Exact percentages: GLUT1, 95.91 \pm 0.5%; GLUT4, 4.09 \pm 0.5%. Data are mean \pm SEM from three independent experiments.

to the hypothesis that serum-derived factors may trigger pathways for glucose metabolism, thus reducing the availability of glucose precursors for HA synthesis. Since stimulation of glycolysis is a well-established metabolic function of insulin, we tested the effects of insulin on glycolysis and HA synthesis. As expected, stimulation with insulin (50 nM) triggered glycolysis, as determined by lowered intracellular G6P levels as well as increased intracellular pyruvate and extracellular lactate concentrations (Fig. 5a). In turn, the amount of HA in the supernatant of the cells was reduced (Fig. 5b).

Accordingly, silencing of the insulin receptor (*INSR*, Fig. 5c) increased the G6P precursor pool, reduced pyruvate and lactate concentrations (Fig. 5d), and strongly triggered HA synthesis (Fig. 5e) independently of changes in HAS transcription (Fig. 5f). Under diabetic conditions, both insulin depletion as found in Type 1 diabetes and insulin resistance, a characteristic feature of Type 2 diabetes, may result in diminished glycolysis and thus yield a larger supply of glucose precursors to HA synthesis. To mimic Type 2 diabetes conditions, we next established a model of experimentally induced insulin resistance in cancer cells, which used prolonged stimulation with insulin to downregulate the downstream signalling of *INSR*, as previously described.²⁰ To validate this approach, we measured the phosphorylation of insulin receptor subunit beta (*INSR*- β) and insulin receptor substrate 1 (*IRS*-1) with immunoblotting after 24 and 96 hr (Fig. 5g). In this experimental setup, short-term insulin stimulation (24 hr, 100 nM) consistently reduced HA synthesis, while simulated insulin resistance (insulin stimulation for 96 hr, 100 nM) led to a pronounced increase in HA production (Fig. 5h). This observation is in agreement with our observations using *INSR* silencing. To preclude any influence of insulin on glucose uptake in this experimental setup, we determined the expression of *GLUT1*, which facilitates basal glucose uptake independently of insulin, and *GLUT4*, which is largely regulated by insulin, by qPCR. Measurements of the mRNA expression of *GLUT1* and *GLUT4* showed that *GLUT1* is the predominantly expressed isoform in OSC1 cells; therefore, it can be assumed that glucose uptake in OSC1 is also largely independent of insulin effects (Fig. 5i).

Augmented HA production in response to hyperglycaemia and insulin depletion promotes the malignant cancer cell phenotype

Elevated HA production has been shown to exhibit tumour-promoting effects. Therefore, we performed experiments regarding the HA-mediated proliferation, invasion, and metastatic potential of OSC1 cells in response to high glucose supply, diminished insulin actions, and inhibition of glycolysis. In addition to a strong mitogenic effect of insulin, we detected a pronounced increase in proliferation with higher glucose supply (Fig. 6a). Next, we measured the invasive potential of OSC1 cells in response to hyperglycaemia and insulin. OSC1 cells exhibited stronger invasion when cultured

in high-glucose, instead of low-glucose, media. Likewise, the presence of insulin reduced invasion (Fig. 6b). Conversely, abrogating insulin signalling and glycolysis by silencing *INSR* or *PFKM* caused increased invasion (Fig. 6c). For detection of anoikis-resistant cells featuring anchorage-independent growth, we evaluated colony formation in a soft agar assay. The largest number of colonies was consistently observed in response to high glucose concentrations and insulin deprivation, the condition with the highest HA synthesis in previous experiments. Of note, insulin treatment in combination with high glucose concentrations yielded fewer but larger colonies than those found under other conditions (Fig. 6d). This observation may be explained by the anabolic effect of insulin in stimulating colony growth. Also, the inhibitory effect of higher HA content on cell-cell interaction and colony agglomeration in colonies lacking insulin may explain this effect. To address the adhesive capability of OSC1 cells in response to hyperglycaemia and insulin, we performed an endothelial cell adhesion assay. The largest number of adherent cells was again found under conditions that increased HA production: hyperglycaemia and insulin depletion (Fig. 6e) and direct (*siPFKM*) and indirect (*siINSR*) inhibition of glycolysis (Fig. 6f). These findings indicate enhanced cancer cell malignancy in response to conditions under which HA production is increased (cf. Figs. 3–5).

Discussion

Revealing the mechanisms behind the connection between the wide-spread diseases diabetes and cancer can lead to new strategies for prevention and targeted therapy.⁴ Here we focus on the metabolic impact of hyperglycaemia and concomitant aberration of insulin signalling on the extracellular matrix component HA, which exhibits crucial functions in tumour progression.²⁶ In our study, we used ESCC cell lines as a model, which have been well characterised with respect to the impact of the extracellular matrix and especially HA on tumour progression.^{19,27,28} Further research is needed to verify these findings in other tumour entities.

First evidence for the dependence of HA production on glucose supply was provided by studies using bacteria²⁹ that have shown increased concentrations of glucose to induce HA production. Moreover, diabetic rats³⁰ as well as patients with Type 1³¹ and Type 2 diabetes^{32,33} exhibit elevated HA levels in the circulating bloodstream and peripheral tissues. Hyperglycaemia-induced HA was identified to impair wound healing in diabetic patients.³⁴ In COS-1 and MCF-7 cells with overexpression of HAS isoforms, it was shown that HA synthesis depends on the availability of its direct precursors UDP-N-acetyl glucosamine and UDP-glucuronic acid.^{35,36} Here we show that HA production in oesophageal cancer cells natively depends on the early glucose metabolite pool. This observation may indicate a proprietary overexpression of *HAS* genes in ESCC cells conceivably providing a survival factor for these cancer cell type.

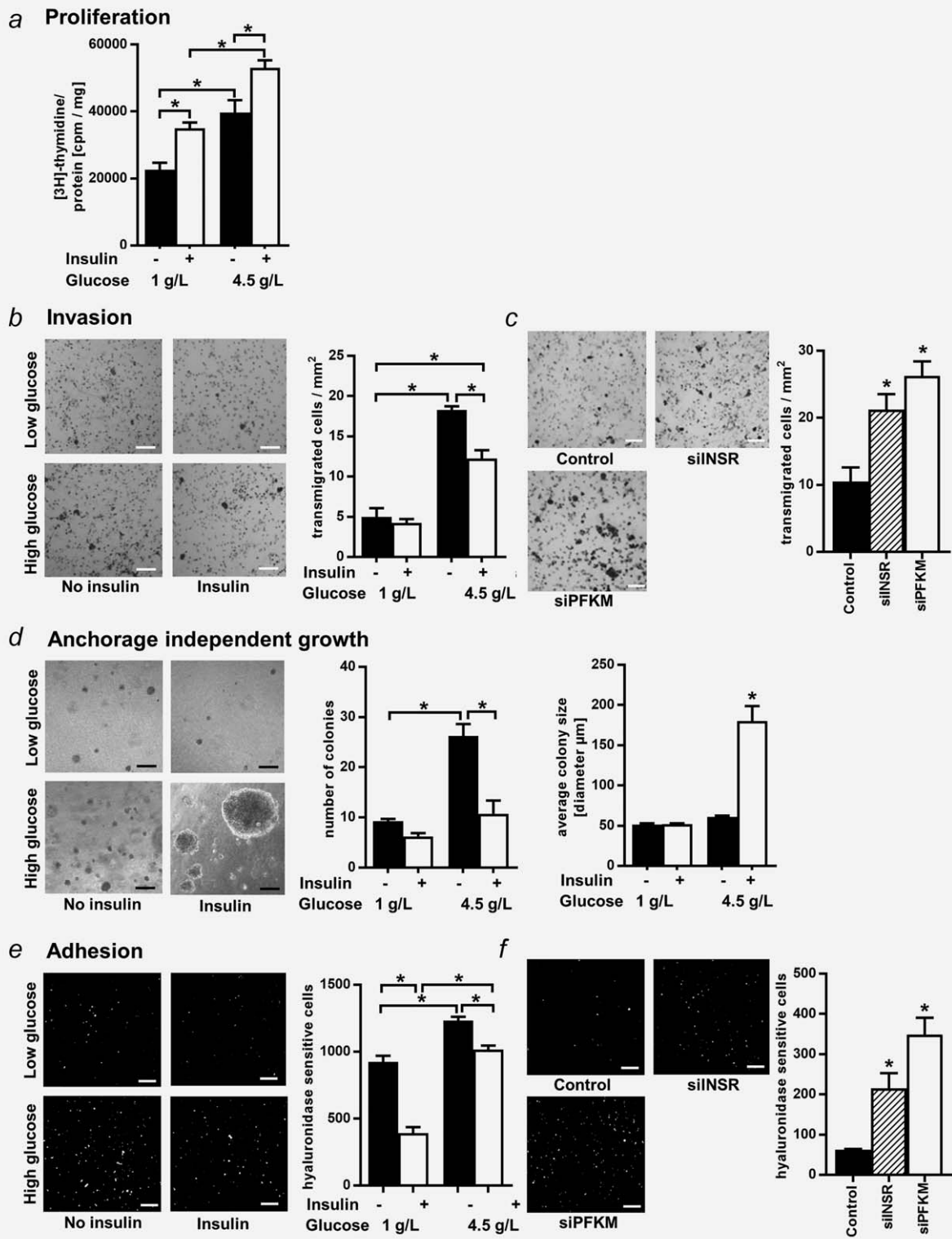


Figure 5. Conditions favouring hyaluronan synthesis cause an increase in proliferation, invasion, anchorage-independent growth and adhesion to endothelial cells *in vitro*. (a) Proliferation of OSC1 cells in response to glucose and insulin (10 μg/ml), as determined by [³H]-thymidine incorporation. Data are mean ± SEM from three independent experiments. *, *p* < 0.05 between indicated conditions. (b) Influence of glucose and insulin (10 μg/ml) on the invasion of OSC1 cells through matrigel. Bar, 200 μm. Data are mean ± SEM from four independent experiments (dark dots: tumour cells, bright dots: pores in the inset membrane). *, *p* < 0.05 vs. indicated condition. (c) Impact of inhibition of glycolysis by silencing of insulin receptor (INSR) and phosphofructokinase M (PFKM) on the invasion of OSC1 cells through matrigel (dark dots: tumour cells, bright dots: pores in the inset membrane). Data are mean ± SEM from four independent experiments. *, *p* < 0.05 vs. control. (d) Anchorage-independent growth of OSC1 cells as determined by colony formation in a soft agar assay. Bar, 200 μm. Data are mean ± SEM from four independent experiments. Number of colonies: *, *p* < 0.05 vs. indicated condition. Average colony size: *, *p* < 0.05 vs. all other conditions. (e) Influence of glucose and insulin (10 μg/ml) on hyaluronan-mediated adhesion of OSC1 cells to endothelial cells. Bar, 200 μm. Data are mean ± SEM from three independent experiments. *, *p* < 0.05 vs. indicated condition. (f) Impact of inhibition of glycolysis by silencing of insulin receptor (INSR) and phosphofructokinase M (PFKM) on hyaluronan-mediated adhesion of OSC1 cells to endothelial cells. Bar, 200 μm. Data are mean ± SEM from three independent experiments. *, *p* < 0.05 vs. control.

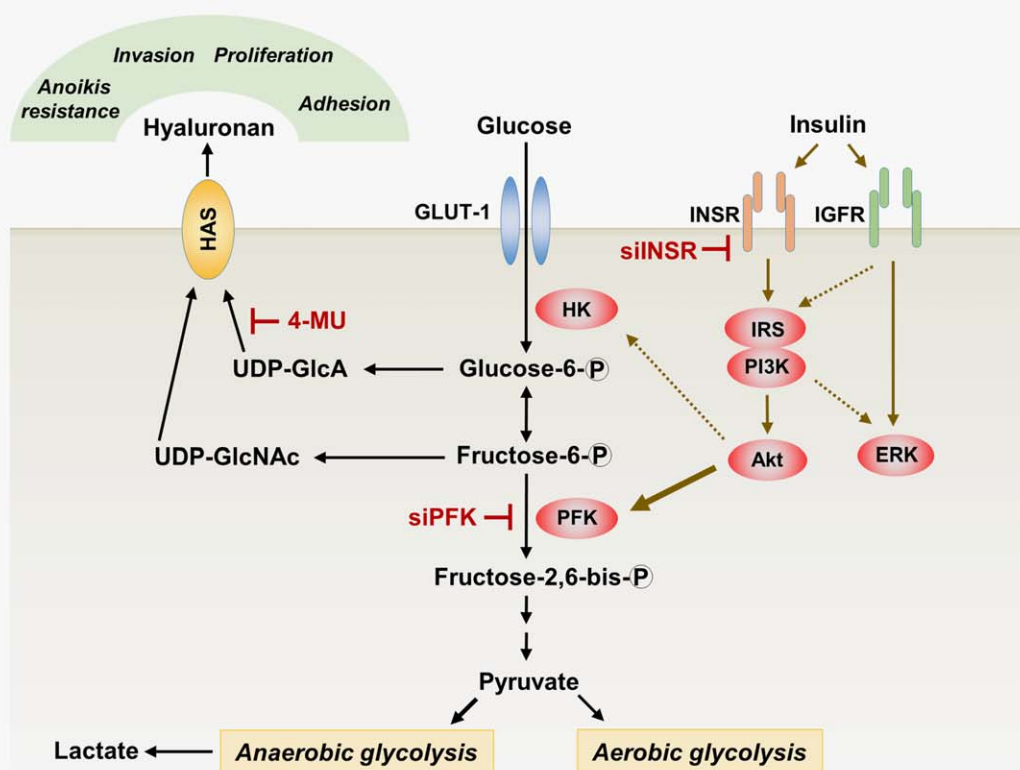


Figure 6. Schematic of interactions between glycolysis and hyaluronan synthesis. Glucose is taken up independently of insulin in most cancer cells by GLUT-1 and is subsequently converted to glucose-6-phosphate (G6P), which is the starting point for glycolysis and the synthesis of HA. Insulin orchestrates the metabolism of glucose toward glycolysis, thus depleting the precursor pool for HA synthesis. The inhibition of glycolysis by abrogated insulin actions or knock down of the glycolytic key enzyme phosphofructokinase (PFK) increases the usage of glucose for HA synthesis, which is inhibited by 4-methylumbelliferone (4-MU). ERK, extracellular signal-regulated kinase; GlcA, glucuronic acid; GlcNAc, N-acetyl-glucosamine; HAS, hyaluronan synthase; HK, hexokinase; IGFR, insulin-like growth factor receptor; INSR, insulin receptor; IRS, insulin receptor substrate; PFK, phosphofructokinase; PI3K, phosphoinositide 3-kinase. [Color figure can be viewed at wileyonlinelibrary.com]

It is important to mention that in most of our experiments the transcriptional regulations of the HAS enzymes do not correspond to the changes in HA synthesis. Most experiments in our study showed that higher HA precursor availability (i.e., hyperglycemia and abrogation of glycolysis by silencing of *INSR*) caused no significant changes in *HAS3* mRNA expression and a decrease in *HAS2* mRNA expression. These findings are in line with recent research on the regulation of HA synthesis showing that the transcriptional control of *HAS2*, its activation and the eventual production of HA is regulated by precursor availability, epigenetic changes in the promoter, O-GlcNAc modifications, ubiquitinations, phosphorylations and translocation to the cell surface.^{37–39} Presumably, these processes are also involved in the regulation of the other HAS isoforms *HAS1* and *HAS3*, this area is under investigation in the HA field. Taken together, current knowledge in this field shows that HAS expression and HA production do not always exhibit a direct relationship, even though HAS mRNA and HAS protein expression show a correlation. In the light of this,

our data indicate that indeed transcriptional changes were not accountable for increased HA synthesis but that an increase of substrates caused an increase of HA. However, it is remarkable that an abrogation of glycolysis by silencing of PFKM resulted in an increase of *HAS3* expression. Therefore, we performed experiments with different PFKM knockdown efficiencies, which showed that *HAS3* mRNA expression is positively correlated with PFKM knockdown efficiency (yielding more substrates for HA synthesis) while there is a trend to a negative correlation with *HAS2* mRNA. In summary, we propose a substrate triggered feedback-loop leading to upregulation of *HAS3* and downregulation of *HAS2* in response to an afflux of glucose precursors.

Importantly, we show that the activity of glycolysis, the main pathway metabolising glucose, counteracts the use of glucose precursors for HA synthesis. Insulin plays a pivotal role in the regulation of glucose homeostasis and proliferation. Thus, aberrant insulin signalling is a crucial characteristic of diabetes. In the context of tumour progression, the two

most important effects of insulin are growth promotion and metabolic regulation of glycolysis.⁴ The anabolic and mitogenic actions of insulin on tumour cells are well documented.⁴⁰ However, the metabolic actions of insulin on tumour progression are not well studied. Concerning glucose metabolism, it is important to differentiate between control of glucose uptake and glycolysis.

Insulin induces glucose uptake in many nonmalignant cells, such as adipocytes and skeletal muscle cells. In most cancer cells, however, glucose uptake is not facilitated by insulin-regulated GLUT-4 but rather by insulin-independent GLUT-1 and, to a lesser degree, by GLUT-3 and other GLUT isoforms.⁴¹ This switch toward uncontrolled glucose uptake is part of the Warburg effect,⁷ which describes a highly enhanced aerobic glycolysis in tumour cells, and also constitutes a hallmark of tumour development that is accompanied by increased aggressiveness of the tumour.⁴² Of note, overexpression of GLUT-1 among patients with ESCC is associated with a poor prognosis and is directly correlated with higher TNM stages.⁴³

Thus, even if insulin may not be necessary for glucose uptake in most cancer cells, it remains an important regulator of glycolysis and proliferation. More precisely, binding of insulin to the INSR, especially subtype B, mediates metabolic effects via the PI3K/Akt pathway, whereas growth processes are promoted by insulin and IGF through the IGF receptor/mitogen-activated protein kinase (MAPK) pathway.^{44,45} These pathways can act independently of each other, e.g., in human muscle cells and adipocytes inhibition of the MAPK pathway does not interfere with the metabolic effects of insulin.⁴⁶ Importantly, there is growing evidence that metabolic and mitogenic pathways triggered by insulin are not only highly separated but that diabetic conditions do not cause a total loss of insulin functions but rather induce a partial or selective insulin resistance with differential regulation of the mitogenic and metabolic pathways.^{47–49} For instance, human skeletal muscle cells of Type 2 diabetes patients exhibiting a reduction of IRS-1 phosphorylation show only a selective reduction in the activity of the metabolic PI3K-Akt-pathway while the mitogenic MAPK pathway remains intact.⁵⁰ These findings imply that the anabolic and therefore growth-promoting effects of insulin can persist, whereas other pathways, such as control of glycolysis, are abrogated. These observations raise the question why an abrogation of glycolysis, eventually resulting in decreased ATP production, might be conducive to tumour cell growth; obviously, this process would be disadvantageous for the energy homeostasis of the cell. However, research on the Warburg effect in cancer cells has provided evidence that cancer cells are prone to use glucose metabolites preferably for biomass gain and other cellular tasks rather than for ATP generation.⁷ Of note, some cancer cells express the dimeric pyruvate kinase M2 protein which diminishes the activity of the glycolytic pathway and thus increases the availability of glucose precursors for use in anabolic pathways.⁵¹

In conclusion, a lack of insulin in untreated Type 1 diabetes, as well as insulin resistance in Type 2 diabetes, may reduce glycolysis, thereby making an increased number of glucose precursors available for production of biomass such as HA synthesis. Simultaneously, proliferation can remain promoted by insulin via INSR-A and IGFR. Indeed, we observed that abrogation of insulin signalling increased the glucose precursor pool and thus stimulated HA synthesis. Concurrently, insulin remains exerted a strong mitogenic effect on the OSC1 cells used in our study. Thus, our results indicate that the tumour-promoting mitogenic actions of insulin, e.g., via the MAPK pathway, combine with increased HA synthesis to further support tumour growth and spread. In line with this, we found an increase in HA-dependent tumour characteristics, i.e., invasion, anchorage-independent growth and adhesion to endothelial cells in response to hyperglycaemia and insulin depletion, conditions favouring HA synthesis.

In this article, we used a nude mouse tumour xenograft model with streptozotocin-induced diabetes to investigate the effects of a diabetic metabolic state on HA-mediated tumour growth. In this model, diabetic conditions produced a pronounced but delayed increase in tumour growth. An explanation for this late onset of growth induction could be that tumour growth in its early stages may depend more on the mitogenic actions conferred by insulin, whereas glucose supply becomes more important in later stages of tumour progression. Two older studies (1972) on tumour growth in diabetic mice reported a decreased growth under diabetic conditions. However, these studies had some critical limitations, i.e., a short observation period, the use of toxic alloxan concentrations, or a pronounced weight loss leading to nutrient depletion also affecting the tumour mass.^{52,53}

Our results show that only in diabetic mice inhibition of HA synthesis by 4-MU caused a higher absolute decrease in tumour volume and significantly reduced proliferation and vessel formation while strongly increasing the fraction of apoptotic cells. In nondiabetic mice, 4-MU delayed the onset of tumour growth resulting in a smaller mean tumour volume at Day 90. However, in this group treatment with 4-MU resulted only in a trend toward less Ki67 and CD31 positive cells and no effects on the TUNEL staining. This observation may be caused by a slower, delayed tumour growth kinetic and a depletion of the HA-rich tumour matrix.

Remarkably, 4-MU treatment also resulted in a pronounced prolongation in survival time of diabetic mice. This effect may be explained by a role of 4-MU in either reduction of tumour burden as a result of diminished HA production, or in a so far unknown amelioration of diabetes-related complications in these mice. However, blood glucose concentrations in diabetic mice were not significantly affected by 4-MU treatment. Further research is needed to specify this interesting effect of 4-MU on the mortality rate associated with diabetic conditions. Notwithstanding, these data indicate that 4-MU may be a promising therapeutic approach for the

treatment of cancer in diabetic patients and may additionally ameliorate diabetes-induced diseases. The fact that 4-MU (INN: hymecromone) is an orally bioavailable small molecular compound drug that has been approved as a spasmolytic in several countries for human use over many decades facilitates further clinical trials.

In summary, here we show that HA production in oesophageal cancer is modulated by glucose supply and by the glycolytic activity controlled by insulin (Fig. 6). We demonstrate the functional relevance of increased HA synthesis in response to hyperglycaemia and insulin depletion for the malignant cancer cell phenotype *in vitro* and for tumour progression and survival *in vivo*. Thus, our findings reveal the

central role of HA metabolism as a link between chronic hyperglycaemia, insulin signalling, and ESCC tumour progression and suggest a future clinical use of HA synthesis inhibitors such as 4-MU as an add-on therapeutic for cancer patients with diabetic comorbidity.

Acknowledgements

S.T. designed the experiments, researched data, and wrote the article. U.P. researched data. C.R., D.J.G. and K.R. researched data and reviewed the article. J.W.F. designed the experiments, contributed guidance and reviewed the article. We appreciate the support by Birte Möhlendick, Tanja Arent, Wolfgang Huckenbeck and Barbara Hildebrandt in validating the cell lines used in our study.

References

- Vigneri P, Frasca F, Sciacca L, et al. Diabetes and cancer. *Endocr Relat Cancer*, 2009;16:1103–23.
- Huang W, Ren H, Ben Q, et al. Risk of esophageal cancer in diabetes mellitus: a meta-analysis of observational studies. *Cancer Causes Control* 2012;23:263–72.
- Feng YH, Lin CY, Huang WT, et al. Diabetes mellitus impairs the response to intra-arterial chemotherapy in hepatocellular carcinoma. *Med Oncol*, 2011;28:1080–8.
- Giovannucci E, Harlan DM, Archer MC, et al. Diabetes and cancer: a consensus report. *Diabetes Care*, 2010;33:1674–85.
- Hanahan D, Weinberg RA. Hallmarks of cancer: the next generation. *Cell*, 2011;144:646–74.
- Warburg O. On the origin of cancer cells. *Science*, 1956;123:309–14.
- Vander Heiden MG, Cantley LC, Thompson CB. Understanding the Warburg effect: the metabolic requirements of cell proliferation. *Science*, 2009;324:1029–33.
- Masur K, Vetter C, Hinz A, et al. Diabetogenic glucose and insulin concentrations modulate transcriptome and protein levels involved in tumour cell migration, adhesion and proliferation. *Br J Cancer*, 2011;104:345–52.
- Cencioni C, Spallotta F, Greco S, et al. Epigenetic mechanisms of hyperglycemic memory. *Int J Biochem Cell Biol*, 2014;51:155–8.
- Ryu TY, Park J, Scherer PE. Hyperglycemia as a risk factor for cancer progression. *Diabetes Metab J*, 2014;38:330–6.
- Pennathur A, Gibson MK, Jobe BA, et al. Oesophageal carcinoma. *Lancet*, 2013;381:400–12.
- Toole BP. Hyaluronan: from extracellular glue to pericellular cue. *Nat Rev Cancer*, 2004;4:528–39.
- Sironen RK, Tammi M, Tammi R, et al. Hyaluronan in human malignancies. *Exp Cell Res*, 2011;317:383–91.
- Lin EW, Karakasheva TA, Hicks PD, et al. The tumor microenvironment in esophageal cancer. *Oncogene*, 2016;35:5337–5349.
- Itano N, Sawai T, Yoshida M, et al. Three isoforms of mammalian hyaluronan synthases have distinct enzymatic properties. *J Biol Chem*, 1999;274:25085–92.
- Kakizaki I, Kojima K, Takagaki K, et al. A novel mechanism for the inhibition of hyaluronan biosynthesis by 4-methylumbelliferone. *J Biol Chem*, 2004;279:33281–9.
- Goalstone ML, Draznin B. Insulin signaling. *West J Med*, 1997;167:166–73.
- Sarbia M, Bosing N, Hildebrandt B, et al. Characterization of two newly established cell lines derived from squamous cell carcinomas of the oesophagus. *Anticancer Res*, 1997;17:2185–92.
- Twarock S, Tammi MI, Savani RC, et al. Hyaluronan stabilizes focal adhesions, filopodia, and the proliferative phenotype in esophageal squamous carcinoma cells. *J Biol Chem*, 2010;285:23276–84.
- Kumar N, Dey CS. Development of insulin resistance and reversal by thiazolidinediones in C2C12 skeletal muscle cells. *Biochem Pharmacol*, 2003;65:249–57.
- Jenkins RH, Thomas GJ, Williams JD, et al. Myofibroblastic differentiation leads to hyaluronan accumulation through reduced hyaluronan turnover. *J Biol Chem*, 2004;279:41453–60.
- Barnes J, Tian L, Loftis J, et al. Isolation and analysis of sugar nucleotides using solid phase extraction and fluorophore assisted carbohydrate electrophoresis. *MethodsX*, 2016;3:251–60.
- Zhang L, Underhill CB, Chen L. Hyaluronan on the surface of tumor cells is correlated with metastatic behavior. *Cancer Res*, 1995;55:428–33.
- Graham ML, Janecek JL, Kittredge JA, et al. The streptozotocin-induced diabetic nude mouse model: differences between animals from different sources. *Comp Med*, 2011;61:356–60.
- Euhus DM, Hudd C, LaRegina MC, et al. Tumor measurement in the nude mouse. *J Surg Oncol*, 1986;31:229–34.
- Itano N, Zhuo L, Kimata K. Impact of the hyaluronan-rich tumor microenvironment on cancer initiation and progression. *Cancer Sci*, 2008;99:1720–5.
- Twarock S, Freudenberger T, Poscher E, et al. Inhibition of oesophageal squamous cell carcinoma progression by *in vivo* targeting of hyaluronan synthesis. *Mol Cancer*, 2011;10:30.
- Twarock S, Rock K, Sarbia M, et al. Synthesis of hyaluronan in oesophageal cancer cells is uncoupled from the prostaglandin-cAMP pathway. *Br J Pharmacol*, 2009;157:234–43.
- Pires AM, Santana MH. Metabolic effects of the initial glucose concentration on microbial production of hyaluronic acid. *Appl Biochem Biotechnol*, 2010;162:1751–61.
- Chajara A, Raoudi M, Delpech B, et al. Circulating hyaluronan and hyaluronidase are increased in diabetic rats. *Diabetologia*, 2000;43:387–8.
- Nieuwdorp M, Holleman F, de Groot E, et al. Perturbation of hyaluronan metabolism predisposes patients with type 1 diabetes mellitus to atherosclerosis. *Diabetologia*, 2007;50:1288–93.
- Dasu MR, Devaraj S, Park S, et al. Increased toll-like receptor (TLR) activation and TLR ligands in recently diagnosed type 2 diabetic subjects. *Diabetes Care*, 2010;33:861–8.
- Kang L, Lantier L, Kennedy A, et al. Hyaluronan accumulates with high-fat feeding and contributes to insulin resistance. *Diabetes*, 2013;62:1888–96.
- Shakya S, Wang Y, Mack JA, et al. Hyperglycemia-induced changes in hyaluronan contribute to impaired skin wound healing in diabetes: review and perspective. *Int J Cell Biol*, 2015;2015:701–38.
- Rilla K, Oikari S, Jokela TA, et al. Hyaluronan synthase 1 (HAS1) requires higher cellular UDP-GlcNAc concentration than HAS2 and HAS3. *J Biol Chem* 2013;288:5973–83.
- Siiskonen H, Karna R, Hyttinen JM, et al. Hyaluronan synthase 1 (HAS1) produces a cytokine- and glucose-inducible, CD44-dependent cell surface coat. *Exp Cell Res*, 2014;320:153–63.
- Hascall VC, Wang A, Tammi M, et al. The dynamic metabolism of hyaluronan regulates the cytosolic concentration of UDP-GlcNAc. *Matrix Biol*, 2014;35:14–7.
- Tammi RH, Passi AG, Rilla K, et al. Transcriptional and post-translational regulation of hyaluronan synthesis. *FEBS J*, 2011;278:1419–28.
- Vigetti D, Viola M, Karousou E, et al. Metabolic control of hyaluronan synthases. *Matrix Biol*, 2014;35:8–13.
- Gallagher EJ, Fierz Y, Ferguson RD, et al. The pathway from diabetes and obesity to cancer, on the route to targeted therapy. *Endocrine Practice*, 2010;16:864–73.
- Medina RA, Owen GI. Glucose transporters: expression, regulation and cancer. *Biol Res*, 2002;35:9–26.
- Hockel M, Vaupel P. Tumor hypoxia: definitions and current clinical, biologic, and molecular aspects. *J Natl Cancer Inst*, 2001;93:266–76.
- Kato H, Takita J, Miyazaki T, et al. Glut-1 glucose transporter expression in esophageal squamous cell carcinoma is associated with tumor aggressiveness. *Anticancer Res*, 2002;22:2635–9.
- Samani AA, Yakar S, LeRoith D, et al. The role of the IGF system in cancer growth and metastasis: overview and recent insights. *Endocrine Rev*, 2007;28:20–47.

45. Nakae J, Kido Y, Accili D. Distinct and overlapping functions of insulin and IGF-I receptors. *Endocrine Rev*, 2001;22:818–35.
46. Lazar DF, Wiese RJ, Brady MJ, et al. Mitogen-activated protein kinase inhibition does not block the stimulation of glucose utilization by insulin. *J Biol Chem*, 1995;270:20801–7.
47. Groop PH, Forsblom C, Thomas MC. Mechanisms of disease: pathway-selective insulin resistance and microvascular complications of diabetes. *Nat Clin Practice Endocrinol Metab*, 2005;1:100–10.
48. Brown MS, Goldstein JL. Selective versus total insulin resistance: a pathogenic paradox. *Cell Metab*, 2008;7:95–6.
49. Parker VE, Savage DB, O'Rahilly S, et al. Mechanistic insights into insulin resistance in the genetic era. *Diabetic Med*, 2011;28:1476–86.
50. Cusi K, Maezono K, Osman A, et al. Insulin resistance differentially affects the PI 3-kinase- and MAP kinase-mediated signaling in human muscle. *J Clin Invest* 2000; 105:311–20.
51. Mazurek S, Boschek CB, Hugo F, et al. Pyruvate kinase type M2 and its role in tumor growth and spreading. *Semin Cancer Biol*, 2005; 15:300–8.
52. Heuson JC, Legros N. Influence of insulin deprivation on growth of the 7,12-dimethylbenz(a)anthracene-induced mammary carcinoma in rats subjected to alloxan diabetes and food restriction. *Cancer Res*, 1972;32:226–32.
53. Puckett CL, Shingleton WW. The effect of induced diabetes on experimental tumor growth in mice. *Cancer Res*, 1972;32:789–90.